Annexin A2 links poor myofiber repair with inflammation and adipogenic replacement of the injured muscle

Annexin A2 links poor myofiber repair with inflammation and adipogenic replacement of the injured muscle

Aurelia Defour[1,2], Sushma Medikayala[1], Jack H Van der Meulen[1], Marshall W Hogarth[1], Nicholas Holdreith[1], Apostolos Malatras[3], William Duddy[3,4], Jessica Boehler[1], Kanneboyina Nagaraju[1,5], Jyoti K Jaiswal[1,5,]*

[1] Center for Genetic Medicine Research, 111 Michigan Av NW, Children's National Health System, Washington D. C. 20010

[2] Current Address: Aix Marseille Université, UMR_S 910, Génétique Médicale et Génomique Fonctionnelle, 13385, Marseille, France

[3] Center for Research in Myology, Sorbonne Universités, UPMC University Paris 06, INSERM UMRS975, CNRS FRE3617, GH Pitié Salpêtrière, Paris 13, France

[4] Northern Ireland Centre for Stratified Medicine, Altnagelvin Hospital Campus, Ulster University, Londonderry, Northern Ireland, UK

[5] Department of Integrative Systems Biology, George Washington University School of Medicine and Health Sciences, Washington, D.C

Author for correspondence:

**Jyoti K. Jaiswal (jkjaiswal@cnmc.org)*

Phone: (202)476-6456; Fax: (202)476-6014

ABSTRACT

Repair of skeletal muscle after sarcolemmal damage involves dysferlin and dysferlin-interacting proteins such as annexins. Mice and patient lacking dysferlin exhibit chronic muscle inflammation and adipogenic replacement of the myofibers. Here we show that similar to dysferlin, lack of annexin A2 (AnxA2) also results in poor myofiber repair and progressive muscle weakening with age. By longitudinal analysis of AnxA2-deficient muscle we find that poor myofiber repair due to the lack of AnxA2 does not result in chronic inflammation or adipogenic replacement of the myofibers. Further, deletion of AnxA2 in dysferlin deficient mice reduced muscle inflammation, adipogenic replacement of myofibers, and improved muscle function. These results identify multiple roles of AnxA2 in muscle repair, which includes facilitating myofiber repair, chronic muscle inflammation and adipogenic replacement of dysferlinopathic muscle. It also identifies inhibition of AnxA2-mediated inflammation as a novel therapeutic avenue for treating muscle loss in dysferlinopathy.

INTRODUCTION

Skeletal muscle responds to minor damage of the myofiber sarcolemma by repair of the damaged membrane. However, myofibers that fail to repair and undergo necrotic death, are replaced through regeneration. Together, repair and regeneration of the injured myofibers enable repair of muscle injury. While myofiber repair involves subcellular processes that occur over minutes following injury, myofiber regeneration involves inflammatory and myogenic processes that occur over hours to days following injury (1,2). Cellular proteins that coordinate myofiber repair and regeneration over this timescale to ensure efficient muscle repair, are poorly understood. Proteins that can coordinate both, myofiber repair and myofiber regeneration *in vivo* should be able to 1) sense and respond to myofiber injury, 2) activate inflammatory and myogenic cells in response to myofiber injury, and 3) facilitate myogenesis to replace necrotic myofibers. Defects in the above processes exacerbate tissue damage and lead to the loss of muscle function, underscoring the need to identify proteins and the mechanisms involved in it.

Annexins are calcium binding proteins that regulate various intracellular events that are altered in muscle diseases (3-7). Recent *in vitro* and *in vivo* studies of myofibers and other cells have found that annexin and their binding partners are recruited to and facilitate repair of plasma membrane (PM) injury (8-13). A role of annexins in myofiber regeneration is supported by our previous analysis of Annexin A1 and by gene expression analysis of muscles acutely injured *in vivo* by cardiotoxin injection, which shows expression of annexins, including annexins A1 and A2 increases immediately following injury and remains elevated for days, during the course of muscle repair (Fig. S1;(14), (15)). In addition to myofiber regeneration, *in vivo* and *ex vivo* analyses show that annexins also mediate tissue inflammation (15-18). Tissue inflammation has

a complex relationship with muscle repair, while acute inflammation is required for myofiber regeneration chronic inflammation causes muscle disease (1). Such muscle diseases include Limb Girdle Muscular Dystrophy (LGMD) 2B and Miyoshi Myopathy (MM), which are caused by mutations in dysferlin gene. Lack of dysferlin compromises repair of myofibers following *ex vivo* sarcolemmal injury, and leads to chronic inflammation, increased muscle degeneration and, gradual adipogenic replacement of myofibers *in vivo* (19-25). Eccentric exercise accelerates disease progression and adipogenic muscle replacement in dysferlinopathic mice and patients (26,27). However, with the link between the incidence of *in vivo* sarcolemmal lesions and dysferlinopathic myofiber degeneration due to myofiber loss and adipogenic replacement being unclear, the basis for dysferlinopathic muscle pathology remains elusive.

Dysferlinopathic muscles show increased macrophages, in addition to CD4+ and CD8+ cells (28,29). While muscle inflammation is required during early phase of muscle repair (30), the basis for increased and chronic inflammation in dysferlinopathy remains enigmatic. Some of the suggested links for poor muscle repair and inflammation in dysferlinopathy include the chemotactic factor thrombospondin 1 (31), TNF-α (32), and complement factor C3 (33). Testing the importance of these links is complicated by discordant effects of reducing muscle inflammation in dysferlinopathy: while use of anti-inflammatory steroid therapy is not beneficial for dysferlinopathy, loss of B and T lymphocytes and loss of Toll-like receptor (TLR)-mediated innate immune response reduces muscle pathology and improves muscle strength (34-36). Thus, to develop anti-inflammatory therapy for LGMD2B there is a need to identify the link between poor myofiber sarcolemmal repair and chronic muscle inflammation. Annexins have been postulated as a regulator of disease in dysferlinopathy as annexins, such as annexin A1 and A2 co-localize and interact with dysferlin in injured muscle cells (13,37). Annexins A1 and A2 are

also increased in LGMD2B patients and mice, in a manner that correlates positively with the severity of their symptoms (6,37,38).

Using AnxA1-null mice we recently identified that AnxA1 deficit does not compromise repair of injured myofibers but slows satellite cell fusion and thus myofiber regeneration (15). Here, we have examined the role of AnxA2 in repair of injured muscles. We have tested the role of AnxA2 in healthy and dysferlin-deficient mouse (B6A/J) muscle using mice lacking AnxA2 (A2) or lacking AnxA2 and dysferlin (B6A/JA2). Similar to dysferlin deficient myofibers, AnxA2-deficient myofibers poorly repair injury to their sarcolemma and show a progressive age-dependent decline in muscle function. However, unlike the dysferlin-deficient muscle, AnxA2-deficient muscles do not exhibit chronic inflammation even as muscle function declines with age. While AnxA2-deficient dysferlinopathic myofibers repair poorly, these muscles exhibit reduced inflammation. This identifies a need for AnxA2 to activate chronic inflammation caused by poor repair. In the absence of AnxA2, dysferlinopathic muscle shows extensive myofiber regeneration, but not degeneration or adipogenic replacement. These reductions in muscle histopathology occur concomitantly with improved muscle strength and *in vivo* muscle function. Thus we identify AnxA2 as a regulator of myofiber repair and muscle inflammation, which facilitates adipogenic conversion of dysferlinopathic muscle and is thus a potential target to treat dysferlinopathy.

RESULTS

Annexin A2 is required for myofiber sarcolemmal repair

With the association of annexin A2 to dysferlin and the role of annexin A2 in PM repair in non-muscle cells (9,37), we examined the PM repair ability of Anx2-deficient (A2) myofibers. To monitor the kinetics of repair, myofibers in intact isolated muscles were injured *ex vivo* by focal laser injury as we previously described (21,39,40). The kinetics of sarcolemmal repair following injury was monitored by measuring the cellular entry of membrane impermeable dye FM1-43. Injury to parental wild type (WT; C57BL/6) and A2 mice showed that lack of AnxA2 reduced the ability of the injured myofibers to repair (Fig. 1A, B). Next, we examined the effect of AnxA2 deficit on repair of myofibers injured mechanically by *ex vivo* lengthening contraction (LC)-induced injury. Using *Extensor Digitorum Longus* (EDL) and *Soleus* (SOL) muscles we monitored the recovery of muscle contractile force and the ability to exclude entry of cell impermeant dye procion orange following repeated LC injury by stretching of 10% for fast (EDL) and slow (SOL) muscle. Both EDL and SOL muscles from A2 mice showed a greater decrease in contractile force following each round of LC injury (Fig. 1C, D). After 9 consecutive LC injuries, A2 EDL muscle showed over 20% greater loss in contractile force as compared to the WT muscle (Fig. 1C). To assess the extent of sarcolemmal injury due to LC-injury, injured EDL muscle was incubated in cell impermeant dye procion orange. Compared to WT EDL muscle, more myofibers in the A2 muscle were labeled with procion orange (Fig. 1E). Thus, use of two independent assays to monitor the repair of injured myofibers shows that, similar to what is known for dysferlin, lack of AnxA2 also reduces the ability of injured myofibers to repair.

Mice lacking Annexin A2 show age-dependent loss of muscle function

Due to the reduced ability of the A2 myofiber to repair sarcolemmal injury, we next assessed the effect of AnxA2 deficit on *in vivo* muscle growth and function. Over the first 9 months of life A2

mice showed similar increase in body and muscle mass as the parental WT, but by 12 months the increase in body mass and muscle mass declined in the A2 animals, but the myofibers did not show concomitant decrease in size, indicating they were not atrophic (Fig. S2A-F). To assess the effect of AnxA2 deletion on muscle strength we performed *in vivo* and *ex vivo* measurements of muscle contractile strength. *In vivo* measurement of the forelimb grip strength showed a decrease in grip strength of A2 mice at 3 months of age and the forelimb continued to remain weaker at all ages tested till 12 months old (Fig. 2A). To assess if there is a potential involvement of neurological effects in the decrease of *in vivo* contractile force, we measured the contractile ability of isolated EDL muscle *ex vivo*. EDL muscle from A2 mice showed a lower force production starting from 3 months of age, but the difference became significant starting from 6 months old and continued to remain weak even thereafter (Fig. 2B). These results indicate that lack of AnxA2 decreases muscle force generation. To assess if the decline in muscle strength is reflected in voluntary physical activity of the A2 animals we measured activity of the mice in an open field behavioral assessment at 3 and 6 months of age. At 3 months of age, the activity of A2 mice was indistinguishable from the WT mice, but by 6 months of age, A2 mice showed a 2 to 5-fold decline in all the activity measures assessed (Fig. 2C-E). Together, these data show that AnxA2 deficit recapitulates the age dependent decrease in muscle strength and physical activity seen in dysferlinopathy.

Lack of Annexin A2 does not cause muscle inflammation and degeneration

In view of the above similarities in the effect of dysferlin and AnxA2 deficit at the cellular and tissue level, we next examined if AnxA2 and dysferlin deficient muscle also exhibit similar changes in gene expression. Principal component analysis of the microarray gene expression data

for the Gastrocnemius (GSC) muscles of 6 months old AnxA2 deficient and parental WT mice (n = 4 per group) showed no clustering of samples into the two genotypes (Fig. S3A). Accordingly, we observed only 6 differentially-expressed genes (including AnxA2) with a false discovery rate (FDR) of < 0.1 (Table S1). To test for accumulation of weak changes across gene sets we carried out gene set enrichment analysis against 2,510 canonical pathways, gene ontology terms, and gene lists derived from previous muscle gene expression studies. This identified 16 gene sets with FDR < 0.1, many of which are related to protein degradation (Fig. S3B). Leading edge analysis suggested this is driven by the up-regulation of a small subset of proteasomal subunit proteins (Fig. S3B, C). This is a modest change in gene expression as compared to the hundreds of genes that show altered expression in recent studies of dysferlin deficient muscles (41-43). Dysferlin deficient muscles show a notable increase in muscle inflammation (44). For a focused analysis of alterations in inflammatory genes between AnxA2 and dysferlin deficient mouse muscles we compared muscle gene expression data obtained from the A2 muscle with complete transcriptomic profiles of 3 recent murine dysferlinopathic muscle studies GSE2629 (41), GSE2507 (42), and GSE2112 (43). None of the inflammation-related gene ontology (GO) terms dysregulated in these dysferlin-deficient datasets were dysregulated in the A2 muscle (Table S2).

To further examine this lack of any remarkable change in inflammatory gene expression in the 6 months old A2 muscle, we performed longitudinal muscle histopathological analysis of the GSC muscle from A2, WT and dysferlinopathic (B6A/J) mice at 3, 6 and 9 months of age (Fig. 3A). In agreement with the gene expression analysis we observed that compared to the dysferlinopathic (B6A/J) muscle, A2 muscles showed relatively little histopathology even at 9 months of age. While compared to the WT muscle, B6A/J GSC muscle showed an increase in the number of degenerating fibers, inflammatory foci and regenerating fibers at all ages (up to

17, 20 and 35-fold respectively at 9 months), A2 muscle do not show any difference (Fig. 3B-D). Thus, despite similar loss in *ex vivo* measures of myofiber repair and muscle function for AnxA2 and dysferlin deficient mice, AnxA2 deficient mice exhibit minimal muscle histopathology and inflammation *in vivo*.

Annexin A2 links poor myofiber repair and dysferlinopathic muscle inflammation

AnxA2 facilitates inflammatory signaling, and increase in AnxA2 expression in dysferlinopathic and regenerating muscle is linked with increased muscle inflammation (6,17,38,45). We thus hypothesized that the lack of A2 muscle inflammation despite poor myofiber repair indicates a requirement of AnxA2 for triggering muscle inflammation. To test this hypothesis we generated mice deficient in dysferlin and AnxA2. As the A2 mice are on the C57BL/6 strain, we cross-bred it with dysferlin deficient mice on the C57BL/6 strain - B6A/J (27). Genotype of the dysferlin/AnxA2 null (B6A/JA2) mice was confirmed as before (21,46) (Fig. S4A, B). The B6A/JA2 mice were viable, with no obvious defect in growth and development (Fig. 4A-C).

To test the ability of myofibers from the B6A/JA2 mice to repair sarcolemmal injury we used the *ex vivo* laser injury assay as described above. PM injury in the B6A/JA2 myofibers resulted in even greater FM dye entry as compared to the B6A/J myofibers, indicating their reduced ability to repair sarcolemmal injury (Fig. 4D). Further, this indicates that AnxA2 helps with repair of the dysferlinopathic myofibers. If the role of AnxA2 in muscle injury was limited to its role in myofiber repair, this observation would predict a worse pathology for B6A/JA2 mice as compared to the B6A/J mice. However, if as per our hypothesis, AnxA2 does indeed link myofiber repair deficit with muscle inflammation, B6A/JA2 mice will have reduced inflammation and thus reduced muscle pathology as compared to B6A/J mice. Since muscle

pathology in B6A/J mouse gets progressively worse at older ages, we examined histology of muscle sections in old (> 18 months) WT, A2, B6A/J and B6A/JA2 mice (Fig. 4E). As previously shown in GSC (Fig 3) there was significantly greater number of degenerating and regenerating fibers, as well as inflammatory foci in the EDL muscle of B6A/J mice as compared to the WT and A2 mice (Fig. 4F-H). However, in comparison to B6A/J muscles, EDL muscles of 18-24 months old B6A/JA2 showed 2 to 7-fold decreases in the number of degenerating fibers, regenerating fibers, and inflammatory foci (Fig. 4F-H). This reduction in muscle pathology was also observed in all the other muscles, namely Tibialis Anterior (TA), GSC, and *Psoas* that were examined (Fig. S5). This identifies that AnxA2 deficit is protective against the muscle degeneration caused by dysferlin deficit.

As an independent assessment of the nature of muscle inflammation, we quantified inflammatory markers for B cell, T cell, macrophages, and TLR-mediated innate immune response, all of which are involved in dysferlinopathy (35,36,47). Using qRT-PCR we assessed expression of B cell marker CD19, T cell markers CD4, CD8A, macrophage marker EMR1 (F4/80), and innate immune signaling (TLR4, IL12, and TNFα). Compared to 18-24 months old WT muscles, these markers were unaltered in age-matched A2 muscles, but up-regulated in age-matched B6A/J muscle (Fig. 4I, J). Compared to B6A/J muscle, B6A/JA2 muscles showed up to 7-fold reduction in expression of B and T lymphocyte markers, and showed a trend for reduced expression of TLR4 as well as TLR-regulated genes IL-12 and TNFα (Fig. 4I, J). However, the expression of the macrophage marker F4/80 (EMR1) was unaltered (Fig. 4I). These results show that lack AnxA2 inhibits inflammation of dysferlin deficient muscles even at late symptomatic stage.

Adipogenic conversion of the dysferlinopathic muscle depends on Annexin A2

Previous studies have shown that dysferlin deficiency in patients and animals results in a significant fatty replacement of muscles cells in age and symptom dependent manner, which may relate to altered inflammatory response due to dysferlin deficit (23,24). To assess appearance of adipogenic signature in muscle we used the transcriptomic profiles of GSC muscle from dysferlinopathic mice (GSE2629 (41), GSE2507 (42), and GSE2112 (43)) for GO terms relating to cellular markers for adipogenic and fatty acid metabolism genes to assess if any of these were dysregulated in muscle of 7 months old dysferlin deficient mice (Table S2). To aid in interpretation of this analysis, we also assessed these GO terms in a dataset comparing adipose tissue to muscle (GSE51866). Adipogenic GO terms dysregulated in 7 months old dysferlin deficient muscle changed similarly to that observed for the fat *versus* muscle comparison; however, similar to the young (< 2 months old) dysferlin deficient muscles, these terms were not dysregulated in AnxA2 deficient muscles. This identifies that adipogenic GO terms that are responsive to disease progression in dysferlin deficient muscle are unaltered in AnxA2 deficient muscle. In agreement with the results from gene expression analysis, histological analysis of one-year old GSC muscle showed obvious signs of adipogenic muscle replacement in dysferlinopathic muscle, while WT and AnxA2 muscle were showed no detectable adipogenic conversion (Fig. 5A). Use of Oil red O staining showed that adipogenic deposits are found within and between myofibers, both of which are missing from age matched GSC muscle from WT and AnxA2 deficient mice. Interestingly, these adipogenic deposits are significantly reduced in B6A/JA2 mice (Fig. 5B). To quantify the extent of adipogenic conversion of muscle we immunostained the muscles with lipid droplet specific protein Perilipin1 which is not abundant in healthy muscle (48). Unlike WT muscles, Perilipin1 staining was abundant in B6A/J muscle,

but lacking in A2 as well as B6A/JA2 muscles (Fig. 5C, D). While the staining was observed both within the myofiber (arrows) and between the myofibers (arrowheads), the little Perilipin1 staining observed in B6A/JA2 muscle rarely occurred within the myofiber.

To assess if the lack of adipogenic replacement of B6A/JA2 muscle is due to a delay (not a block) in adipogenic conversion of muscle we further investigated multiple muscles by H&E and Oil Red O staining (Fig. S4C, S5). These staining showed that there is a gradation of adipogenic replacement of dysferlinopathic muscle with *Psoas*, and GSC muscles being more affected than EDL and TA (Fig. 4E, S4C). Similar to the EDL muscles from two-year old B6A/J mice, which showed reduced histopathology in AnxA2 and in B6A/JA2 muscle (Fig. 4E), we observed consistently reduced lipid deposition in all B6A/JA2 muscles when compared to B6A/J (Fig. S5). In view of the poor myofiber repair of B6A/J and B6A/JA2 muscles, but protection of B6A/JA2 muscle from adipogenic replacement, this demonstrates the requirement of AnxA2 to trigger adipogenic conversion of dysferlin deficient myofibers.

Lack of Annexin A2 improves dysferlinopathic muscle function

Due to the reduced inflammation and adipogenic conversion of muscle we hypothesized that AnxA2 deficiency may improve dysferlinopathic muscle function. We first tested if AnxA2 and dysferlin deficient muscle show improved muscle strength *in vivo*. To assess muscle contractile ability we measured the forelimb and hindlimb grip strength at pre-symptomatic (< 6 months old) and late symptomatic (> 20 months old) B6A/J and B6A/JA2 mice. B6A/JA2 showed a significantly slower decline in grip strength of both the limbs as the disease progressed. While the grip strength of both limbs was similar between pre-symptomatic B6A/J and B6A/JA2 mice, B6A/JA2 mice showed significantly greater grip strength than B6A/J muscle at the late

symptomatic age (Fig. 6A, B). As the decline in muscle strength in late symptomatic B6A/JA2 mice occurs despite poor myofiber sarcolemmal repair (Fig. 4D), we assessed if this is due to an improved ability of the asymptomatic and early symptomatic B6A/JA2 muscles to withstand injury. To test this we subjected 6 and 12 months old EDL muscle from B6A/J and B6A/JA2 mice to *ex vivo* eccentric injury by repeated 10% LC. At both these ages we observed that the EDL muscles from B6A/JA2 mice were more resistant to damaging effects of LC injury, resulting in reduced loss in contractile force upon successive LC injuries (Fig. 6C). The improved resistance of B6A/JA2 EDL muscles to LC injuries is not due to an increase in the strength of the EDL muscle as shown by similar maximal EDL contractile force of B6A/J and B6A/JA2 at pre-symptomatic, as well as early and late symptomatic ages (Fig. 6D).

With the improved function and reduced adipogenic conversion of the B6A/JA2 muscle, we tested if this reflects in the functional measures of activity of the mice. For this we performed open-field measurements of activities of mice at early-symptomatic (≤ 6 months) and late-symptomatic (> 20 months) age. As compared to B6A/J mice, B6A/JA2 mice displayed significantly increased activity in all the measures tested, including total vertical and horizontal activities, as well as total number of all voluntary movements (Fig. 6 E-G), as a level similar or close to WT animals. All the measures of voluntary activities were noticeably improved at both stages, such that B6A/JA2 mice showed increased movement by 50% at early age and 20% at late age (Fig. 6F) and vertical activity was improved by as much as 3-fold in early-symptomatic stage and increased to 6-fold by late-symptomatic stage (Fig. 6E). Taken together, analysis of muscle function and voluntary activities demonstrate that the reduced muscle pathology in the B6A/JA2 mice results in improved functional performance of these mice offering a strong indication in support of functional benefits of AnxA2 deficiency in dysferlinopathic muscle.

DISCUSSION

Muscular dystrophies such as LGDM2B and Miyoshi Myopathy are characterized by poor myofiber repair, exhibit chronic muscle inflammation and degeneration (19,22,23,25,46). Dysferlin, the protein mutated in LGMD2B and MM, interacts with AnxA1, and AnxA2, and is required for sarcolemmal repair (37). Studies in *C. elegans* have underlined the importance of dysferlin interaction with annexins in sarcolemmal repair (13). Annexin A6 has been the only annexin implicated so far in sarcolemmal repair in mammals (4). Mutation of AnxA6 was recently identified to worsen muscle repair and pathology in a dysferlinopathic mouse model (49). Our recent analysis of AnxA1 deficient mice identified that instead of facilitating sarcolemmal repair, AnxA1 facilitates myoblast fusion required for the regeneration of injured myofibers (15). Similar to the role of AnxA1 in non-muscle cells, we have found that AnxA2 is required for repairing injury to the plasma membrane (9,12). Here we show that AnxA2 is also required for the repairing injured mouse myofibers. Our studies with AnxA2 identified that AnxA2 helps with plasma membrane repair by facilitating F-actin buildup at the site of injury (9). F-actin buildup has also been shown to facilitate repair of injured myofibers (8,50). In light of the ability of AnxA2 to interact with F-actin and with dysferlin, it is plausible that AnxA2 facilitates sarcolemmal repair by facilitating F-Actin buildup and dysferlin recruitment at the injured plasma membrane (50). However, with the role of AnxA2 in aggregating and fusing membranes, AnxA2 may also facilitate fusion of dysferlin containing membranes at the site of cell membrane injury (3,50).

Similar to dysferlin, lack of AnxA2 also causes poor myofiber repair and progressive decline in muscle function. However, AnxA2 deficiency does not cause inflammation, or lead to

degeneration of the muscles, identifying AnxA2 as the protein that regulates myofiber repair as well as injury-triggered muscle inflammation. Dysferlinopathic patient muscles show adipogenic replacement of myofibers and increasing disease severity with increasing level AnxA2 in the muscle (6,23,26). Such a role of AnxA2 is further supported by previous reports showing that AnxA2 expression is increased rapidly following injury of healthy muscle, and during the course of disease progression in dysferlinopathic patients (6,14,37,38). These two distinct roles of AnxA2 may be linked to the two distinct localizations of AnxA2 – intracellular (for membrane repair) and extracellular (for activating inflammation). Despite lacking a signal peptide, AnxA2 is secreted by cells in a variety of tissues where AnxA2 binds cell surface receptors (51). Extracellular AnxA2 activates inflammation by regulating shedding of pro-tumor necrosis factor-alpha and by functioning as a ligand of TLR4 (17,45,52). Activation of classical innate immune response due to poor repair of dysferlinopathic myofiber has been shown to play a role in disease progression (33). Additionally, poor cell membrane repair is also proposed to activate alternate innate immune signaling through the release of Danger Associated Molecular Patterns (DAMPs) (53). One such DAMP is the high mobility group 1 (HMGB1) protein which, similar to AnxA2, resides in the cell and upon secretion activates inflammation (54). A role of HMGB1 as a DAMP has been proposed for dystrophin deficient muscle, but protein(s) responsible for activating innate immune response in dysferlinopathy has not been identified. This role of AnxA2 is supported by the reduced expression of TLR-regulated genes in AnxA2 deficient muscle.

In addition to muscle inflammation, a recently identified feature of dysferlinopathic patient and mouse muscle is adipogenic replacement of myofibers (23). Adipogenic replacement of muscle is a feature of symptomatic patient muscles, which is exacerbated by eccentric exercise-induced muscle injury (23,26). Adipogenic replacement of muscle correlates with the

onset of muscle weakness and enhancing disease severity enhances fatty deposition in dysferlinopathic muscles (24,55). Thus, a viable therapeutic approach to treat dysferlinopathy is one which can minimize muscle adipogenic conversion. It was suggested that adipogenic pathology in dysferlin-deficient muscle is regulated by transcription factor CCAAT/enhancer binding protein-δ. By deletion of AnxA2 in dysferlinopathic muscle here we have identified AnxA2 is necessary for adipogenic conversion of dysferlin deficient myofibers. It is worth noting that AnxA2 knockout reduces inflammation and adipogenic conversion of dysferlin deficient muscle despite poor myofiber repair ability. Deletion of AnxA2 in dysferlin deficient mice (B6A/JA2 mice) lowers the level of TLR4 and other inflammatory mediators (Fig. 4). Recently, importance of TLR signaling for dysferlinopathic muscle pathology was uncovered by the knockout of Myd88 - the central facilitator of TLR signaling, which reduced histopathology and improved dysferlinopathic muscle function (36). By identifying that loss of AnxA2 improves dysferlinopathic muscle function, here we show AnxA2 functions as a link between poor myofiber repair and ensuing inflammation and adipogenesis in dysferlinopathic muscle. It appears to do so by linking muscle injury and TLR4-mediated chronic muscle inflammation with subsequent adipogenic replacement of dysferlinopathic myofibers (Fig. S6). Future studies using inflammatory and non-inflammatory cell-specific AnxA2 knockout will help determine the relative contribution of muscle and inflammatory cells in adipogenic replacement of dysferlin-deficient muscle and the nature of the signal that leads to myofiber adipogenesis. The observation that AnxA2 deficit breaks the link between poor myofiber repair and dysferlinopathic muscle pathology provides direct evidence that approaches to prevent adipogenic conversion of dysferlinopathic muscle can be therapeutic even when myofiber repair is deficient. Additionally, in view of the link between muscle adipogenic conversion and clinical

severity in dysferlinopathy it identifies blocking AnxA2 function as a potential therapy for dysferlinopathy. Insight into the mechanism by which AnxA2 links dysferlin deficit to dysferlinopathic muscle degeneration will help unravel the mechanism by which muscle injury, inflammation and adipogenesis are coordinated in dysferlinopathy and provide additional avenues for developing therapies for dysferlinopathy.

MATERIALS AND METHODS

Animal: Methods involving animals were approved by the local institutional animal research Committee and animals were maintained in a facility accredited by the American Association for Accreditation of Laboratory Animal Care. Wild type (WT) mice (C57BL/6) were obtained from Jackson Laboratory (Bar Harbor, ME), annexin A2 knockout mice (A2) were a gift of Dr. Katherine Hajjar from Cornell University Medical Center (New York) and dysferlin deficient mice (B6A/J) were a gift of Dr. I Richard from Genethon (Paris). To generate mice lacking both dysferlin and annexin A2 (B6A/JA2), B6A/J mice were crossed with A2 mice. Homozygous null mice for annexin A2 and dysferlin were obtained in F2 generation and genotyped as described below.

PCR genotyping: To assess the status of both dysferlin null allele and annexin A2 null allele, genomic DNA was PCR amplified as described before by (21) for dysferlin allele and (46) for annexin A2 allele (Fig. S4). The primers used to identify dysferlin mutation (A/J Etn insertion in intron 4) were: dysf-F, 5'-TTCCTCTCTTGTCGGTCTAG-3'; dysf-R, 5'-CTTCACTGGGAAGTATGTCG-3'; ETn-oR, 5'-GCCTTGATCAGAGTAACTGTC-3' and for

annexin A2 allele: A2WT, 5'-GCACAGCAATTCATCACACTAATGTCTTCTTG-3'; A2KO, 5'-GCTGACTCTAGAGGATCCCC-3'; Anint, 5'-TGCGCCACCACGCCCGGCTT GTGCTTGCCAC-3'.

***Ex vivo* cell membrane injury:** *Extensor Digitorum Longus* (EDL) or *Soleus* (SOL) muscle were surgically isolated from euthanized WT, A2, B6A/J and B6A/JA2 mice in Tyrode's solution and laser injury was carried out as described (39) in the Tyrode's buffer containing 1.33 mg/ml FM1-43 dye. The kinetics of repair was determined by measuring the cellular FM1-43 dye fluorescence. FM-dye intensity ($F-F_0$ where F_0 is the original value) was used to quantify the kinetics of cell membrane repair and represented with intervals of 5 frames.

***Ex vivo* force contraction:** Mice at the age of 3, 6, 9, 12 and/or 24 months were anesthetized with intraperitoneal injections containing ketamine (100 mg/kg) and xylazine (10 mg/kg). From the right hindlimb, EDL muscle was dissected and brought into a bath containing Ringer solution (composition in mM: 137 NaCl, 24 $NaHCO_3$, 11 glucose, 5 KCl, 2 $CaCl_2$, 1 $MgSO_4$, 1 NaH_2PO_4, and 0.025 turbocurarine chloride) at 25ºC that was bubbled with a mixture of 95%O_2 and 5%CO_2. With 6-0 silk suture, the proximal tendon was tied to a fixed bottom plate and the distal tendon was tied to the arm of a force transducer (Aurora Scientific, Ontario, Canada, model 305B). The muscle was surrounded by two platinum electrodes to stimulate the muscle. The optimal length of the muscle was established using single 0.2 ms square stimulation pulses. At optimal length, with tetani 300 ms in duration and at frequencies of 30, 100, 150, 200, 220 and 250 Hz, each separated by 2 min intervals, the maximal force of the EDL was measured and normalized for the muscle cross section area. After measuring the length of the muscle with calipers, the muscle was removed from the bath and weighed. The cross section was calculated

based on muscle mass, fiber length and muscle tissue density. Fiber length was determined based on the ratio of fiber length to muscle length of 0.45 (56). The same procedure was repeated for SOL muscle from the right hind limb, but the stimulation duration was 1000 ms at frequencies of 30, 50, 80 and 100 Hz. The fiber length to muscle length for the SOL muscle was 0.71. Before removing the EDL or SOL muscle from the bath, the muscle was subjected to a protocol of lengthening contractions. At optimal length, the EDL muscle was stimulated at 250 Hz for 300 ms until a plateau of maximal force generation was reached. From this plateau, with the muscle stimulated, the muscle was lengthened over 10% of its length with a velocity of 2 fiber lengths per second after which the muscle was passively returned to the optimal length. This was repeated 9 times with 1 min interval between the lengthening contractions. The same procedure was repeated for the SOL muscle, but the muscle was stimulated for 1000 ms at 100 Hz and the muscle was lengthened over 10% its length. After removal of the SOL muscle, the mice were euthanized by CO_2 asphyxiation.

Procion orange staining: After performing the *ex vivo* lengthening contraction injury muscles were placed in 0.2% procion orange dye solution (in Ringer's) for 1 hour at room temperature. After removing the excess dye by washing with Ringer's solution, the muscle was immediately frozen using isopentane pre-chilled in liquid nitrogen. Frozen tissues were sectioned (8 μm) and imaged under red channel using a Nikon Eclipse E800 (Nikon, Japan) microscope that was fitted with a SPOT digital color camera with SPOT advanced software (Diagnostic Instruments, Sterling Heights, MI). Representative pictures (20X) were taken and procion orange positive fibers/image were measured for each section.

Grip strength measurement: At 3, 6, 9, 12 and > 20 months, forelimb and hindlimb grip strength were performed in the morning hours with Grip Strength Meter (GSM, Columbus instruments, Columbus, USA) as described (57). The absolute GSM values (Kgf) for each measurement were used for analysis. The grip strength measurements were collected over a 5-day period after a period of acclimation of 5 days.

Open-field behavioral activity measurements (Digiscan): At 3, 6 and > 20 months, voluntary locomotor activity (movement number, horizontal activity and vertical activity) was measured using an open field digiscan apparatus (Omnitech Electronics, Columbus, Ohio, USA) as described previously (57). Locomotor activity data were collected over a 1-hour period in the morning hours over a 4 consecutive days with a previous period of acclimation of 4 days.

Expression profiling: Directly following euthanasia, *Gastrocnemius* (GSC) muscles from the left hindlimb were directly frozen liquid nitrogen and stored at -80˚C. Total RNA was extracted from frozen *GSC* muscles using Trizol reagent (Life Technologies, USA) and cleaned up with RNeasy MinElute cleanup kit (Qiagen, USA) according to the manufacturers' instructions, and then stored at -80^{o}C until use. RNA samples were analyzed with GeneChip Mouse Genome 430 2.0 microarrays (Affymetrix, Santa Clara, CA). An aliquot of 250 ng of total high-quality RNA from each sample was used. cDNA and biotinylated cRNA were synthesized using the *Affymetrix* GeneChip® 3' IVT Express Target Amplification, Labeling and Control Reagent kit according to manufacturer's instructions. 15.2 ug of biotinylated cRNA was fragmented and hybridized to Affymetrix Gene-Chips MG 430 2.0 for 16 hours. The arrays were washed and stained on the Affymetrix Fluidics station 400 and scanned with a Hewlett Packard G2500A gene Array Scanner according to manufacturer's protocol.

Bioinformatics functional analyses: For datasets for which raw chip image files were available (A2, GSE2507, GSE51866), the following analysis pipeline was followed: (1) microarray quality control was carried out by checking the % present, average background, scale factors and GAPDH and actin 3'::5' ratios for each chip using the affyQCReport R package from Bioconductor (58), and by NUSE and RLE analysis as described previously (59); (2) robust multichip averaging (RMA), consisting of background adjustment, quantile normalization and probeset summarization (60); (3) the characteristic direction geometrical approach was then used to identify differentially expressed genes (DEGs) (61). For dataset GSE2629, raw chip image files were unavailable, so characteristic direction analysis was run on the expression matrix provided by that study's authors, after log2 transformation. For dataset GSE2112, only a published list of differentially expressed genes with fold-changes and p-values was available. For calculation of FDR q-values for the A2 dataset (since characteristic direction does not give a measure of significance), a separate differential expression analysis was carried out using NIA Array Analysis (62). For the A2 dataset, principal component analysis (PCA) was carried out using TM4: Multi-experiment Viewer (63). Rank-based gene set enrichment tests were done using GSEA (64) on normalized, non-log2, gene expression values, applying default settings (e.g. permutations on phenotype, collapse genes to max of probesets) except that minimum overlap with gene sets was changed from 15 to 8 to allow for the small sizes of some dysferlin-related muscle gene sets. Gene Sets were taken from the Muscle Gene Sets homepage (Muscle Gene Sets v1) http://sys-myo.rhcloud.com/muscle_gene_sets.php and from MSigDB http://software.broadinstitute.org/gsea/msigdb/. Gene set enrichment mapping was generated using Cytoscape (65) and Enrichment Map (66). Enrichment tests for inflammation-related and fat-related gene ontology terms were carried out on the most differentially expressed 250 genes

from each comparison, using Enrichr (67). The gene expression data are publicly available from the Gene Expression Omnibus (GEO), series number GSE87557. https://www.ncbi.nlm.nih.gov/geo/query/acc.cgi?acc=GSE87557

Histopathology scoring: Directly following euthanasia, GSC or EDL muscles from the left hindlimb were removed and embedded in OCT and snap frozen in liquid nitrogen-cooled isopentane. For histological analysis, muscles embedded in OCT were subsequently sectioned and stained with haematoxylin and eosin (H&E) as far as possible using the TREAT-NMD guidelines for the DMD mouse (http://www.treat-nmd.eu/research/preclinical/dmd-sops/). The slides were acquired at 40X magnification with Nanozomer microscope (Hamamatsu, Japan) or with VS120 (Olympus, USA) with OlyVIA software, and myofibers in muscle section were assessed for the following features: central nuclei/muscle, regenerating (centrally nucleated) fibers/muscle, and degenerating and necrotic myofibres (that show microscopic evidence of structural damage to the myofibers such as hypercontraction and fragmented sarcoplasm that is accompanied with or without the inflammatory cell invasion) using Image J (NIH).

Quantitative RT-PCR: Directly following euthanasia, GSC muscles from the left hindlimb were directly frozen liquid nitrogen and stored at -80˚C. To isolate RNA for qRTPCR analysis, frozen GSC muscles were homogenized in Trizol (Life technologies) with homogenizer according to manufacturer's instructions. After RNA isolation, RNA was quantified on a Nanodrop N1000 spectrophotometer and a total of 300 ng of RNA was used to produce cDNA using ABI High Capacity cDNA Kit (Thermofisher). Taqman mouse primers were used: CD19, CD4, CD8A, EMR1, IL12, TLR4, TNFα and HRPT (Thermofisher). All qRTPCR reactions were prepared according to manufacturer's instructions using ABI Taqman Gene Expression

Master Mix (Thermofisher) and measured on ABI 7900HT Fast-Time PCR System through SDS 2.4 software. Relative gene expression was calculated using the ΔCt method, with HRPT as the internal reference gene with RQ Manager 1.2.1 software.

Lipid staining: To monitor the presence of lipids, Oil red O staining was performed with 8 µm frozen sections from the GSC of 12 months old WT, A2, B6A/J and B6A/JA2 (n = 3 animals per group) using a commercial staining kit (American MasterTech, Lodi CA, USA), as per manufacturer instructions. To quantify skeletal muscle lipid deposition, frozen 8 µm GSC sections were fixed with chilled 4% paraformaldehyde and incubated with anti-perilipin A/B (Sigma Aldrich; Cat #: P1873) at 5 µg/mL in PBS-Tween with 1% BSA and 10 % goat serum. Perilipin staining was visualized using goat ant-rabbit conjugated to A568 (4 µg/mL, ThermoFisher) and co-stained with A488-conjugated wheat germ agglutinin (2 µg/mL, ThermoFisher) to mark sarcolemmal membranes. Sections were mounted with ProLong Gold including DAPI and imaged using a VS120 slide scanner (Olympus). Perilipin images were thresholded in MetaMorph, and the number and average size of perilipin-positive foci in the entire section was quantified using the program's Integrated Morphometry Analysis.

Statistics: Unless otherwise stated, all analyses were performed using GraphPad Prism version 5. Normality test was assessed for each measurement. Value which was < or > average ± 2 standard deviation was removed. Data are presented as means ± S.E.M. or as medians ± extreme values through whisker plot. Statistical analyses were performed using Student's t-test, ANOVA or Kruskal Wallis test for each age-matched data. Nominal statistical signifance was set at $p \leq 0.05$.

ACKNOWLEDGEMENTS

We would like to thank Drs. Katherine Hajjar and Isabelle Richard for the gift of AnxA2 and dysferlin deficient mice. Drs. Yi-Wen Chen, Jigna Narola, and Zuyi Wang for help with gene expression profiling and Travis Kinder for help with qRT-PCR. This work was supported by grants from National Institute of Arthritis and Musculoskeletal and Skin diseases (grant number R01AR055686) and Muscular Dystrophy Association (grant number MDA277389) to JKJ, from Association Française contre les Myopathies to AD, and from National Institute of Health (grants number K26OD011171, R24HD050846, P50AR060836, U54HD071601) to KN. The microscopy facility is supported by DC-IDDRC National Institute of Health grants (grant number P30HD040677, U54HD090257).

AUTHOR CONTRIBUTIONS

AD, KN, and JKJ conceived the study, AD and JKJ designed the study, AD pursued experiments and analyzed all the data with help from SM, who characterized the A2 mouse, JVM who performed mouse physiology experiment, and MH who performed adipogenesis experiment, JB performed RT-qPCR and NH analyzed tissue histology. The bioinformatics analysis was performed by AM and WD. AD and JKJ wrote the manuscript with help from all the authors.

CONFLICT OF INTEREST

The authors declare no conflict of interest.

REFERENCES

1. Tidball,J.G. (2005) Inflammatory processes in muscle injury and repair. *Am. J. Physiol Regul. Integr. Comp Physiol*, **288**, R345-R353.

2. McNeil,P.L., Khakee,R. (1992) Disruptions of muscle fiber plasma membranes. Role in exercise-induced damage. *Am. J. Pathol.*, **140**, 1097-1109.

3. Gerke,V., Creutz,C.E., Moss,S.E. (2005) Annexins: linking Ca2+ signalling to membrane dynamics. *Nat. Rev. Mol. Cell Biol.*, **6**, 449-461.

4. Swaggart,K.A., Demonbreun,A.R., Vo,A.H., Swanson,K.E., Kim,E.Y., Fahrenbach,J.P., Holley-Cuthrell,J., Eskin,A., Chen,Z., Squire,K.*, et al.* (2014) Annexin A6 modifies muscular dystrophy by mediating sarcolemmal repair. *Proc. Natl. Acad. Sci. U. S. A*, **111**, 6004-6009.

5. Probst-Cousin,S., Berghoff,C., Neundorfer,B., Heuss,D. (2004) Annexin expression in inflammatory myopathies. *Muscle Nerve*, **30**, 102-110.

6. Cagliani,R., Magri,F., Toscano,A., Merlini,L., Fortunato,F., Lamperti,C., Rodolico,C., Prelle,A., Sironi,M., Aguennouz,M.*, et al.* (2005) Mutation finding in patients with dysferlin deficiency and role of the dysferlin interacting proteins annexin A1 and A2 in muscular dystrophies. *Hum. Mutat.*, **26**, 283.

7. Selbert,S., Fischer,P., Menke,A., Jockusch,H., Pongratz,D., Noegel,A.A. (1996) Annexin VII relocalization as a result of dystrophin deficiency. *Exp. Cell Res.*, **222**, 199-208.

8. Demonbreun,A.R., Quattrocelli,M., Barefield,D.Y., Allen,M.V., Swanson,K.E., McNally,E.M. (2016) An actin-dependent annexin complex mediates plasma membrane repair in muscle. *J. Cell Biol.*, **213**, 705-718.

9. Jaiswal,J.K., Lauritzen,S.P., Scheffer,L., Sakaguchi,M., Bunkenborg,J., Simon,S.M., Kallunki,T., Jaattela,M., Nylandsted,J. (2014) S100A11 is required for efficient plasma membrane repair and survival of invasive cancer cells. *Nat. Commun.*, **5**, 3795.

10. Bouter,A., Gounou,C., Berat,R., Tan,S., Gallois,B., Granier,T., d'Estaintot,B.L., Poschl,E., Brachvogel,B., Brisson,A.R. (2011) Annexin-A5 assembled into two-dimensional arrays promotes cell membrane repair. *Nat. Commun.*, **2**, 270.

11. Babiychuk,E.B., Monastyrskaya,K., Potez,S., Draeger,A. (2009) Intracellular Ca(2+) operates a switch between repair and lysis of streptolysin O-perforated cells. *Cell Death. Differ.*, **16**, 1126-1134.

12. McNeil,A.K., Rescher,U., Gerke,V., McNeil,P.L. (2006) Requirement for annexin A1 in plasma membrane repair. *J. Biol. Chem.*, **281**, 35202-35207.

13. Roostalu,U., Strahle,U. (2012) In vivo imaging of molecular interactions at damaged sarcolemma. *Dev. Cell*, **22**, 515-529.

14. Zhao,P., Seo,J., Wang,Z., Wang,Y., Shneiderman,B., Hoffman,E.P. (2003) In vivo filtering of in vitro expression data reveals MyoD targets. *C. R. Biol.*, **326**, 1049-1065.

15. Leikina,E., Defour,A., Melikov,K., Van der Meulen,J.H., Nagaraju,K., Bhuvanendran,S., Gebert,C., Pfeifer,K., Chernomordik,L.V., Jaiswal,J.K. (2015) Annexin A1 Deficiency does not Affect Myofiber Repair but Delays Regeneration of Injured Muscles. *Sci. Rep.*, **5**, 18246.

16. Bizzarro,V., Fontanella,B., Franceschelli,S., Pirozzi,M., Christian,H., Parente,L., Petrella,A. (2010) Role of Annexin A1 in mouse myoblast cell differentiation. *J. Cell Physiol*, **224**, 757-765.

17. Swisher,J.F., Khatri,U., Feldman,G.M. (2007) Annexin A2 is a soluble mediator of macrophage activation. *J. Leukoc. Biol.*, **82**, 1174-1184.

18. Sugimoto,M.A., Vago,J.P., Teixeira,M.M., Sousa,L.P. (2016) Annexin A1 and the Resolution of Inflammation: Modulation of Neutrophil Recruitment, Apoptosis, and Clearance. *J. Immunol. Res.*, **2016**, 8239258.

19. Bansal,D., Miyake,K., Vogel,S.S., Groh,S., Chen,C.C., Williamson,R., McNeil,P.L., Campbell,K.P. (2003) Defective membrane repair in dysferlin-deficient muscular dystrophy. *Nature*, **423**, 168-172.

20. Laval,S.H., Bushby,K.M. (2004) Limb-girdle muscular dystrophies--from genetics to molecular pathology. *Neuropathol. Appl. Neurobiol.*, **30**, 91-105.

21. Defour,A., Van der Meulen,J.H., Bhat,R., Bigot,A., Bashir,R., Nagaraju,K., Jaiswal,J.K. (2014) Dysferlin regulates cell membrane repair by facilitating injury-triggered acid sphingomyelinase secretion. *Cell Death. Dis.*, **5**, e1306.

22. Gallardo,E., Rojas-Garcia,R., de,L.N., Pou,A., Brown,R.H., Jr., Illa,I. (2001) Inflammation in dysferlin myopathy: immunohistochemical characterization of 13 patients. *Neurology*, **57**, 2136-2138.

23. Grounds,M.D., Terrill,J.R., Radley-Crabb,H.G., Robertson,T., Papadimitriou,J., Spuler,S., Shavlakadze,T. (2014) Lipid accumulation in dysferlin-deficient muscles. *Am. J. Pathol.*, **184**, 1668-1676.

24. Terrill,J.R., Radley-Crabb,H.G., Iwasaki,T., Lemckert,F.A., Arthur,P.G., Grounds,M.D. (2013) Oxidative stress and pathology in muscular dystrophies: focus on protein thiol oxidation and dysferlinopathies. *FEBS J.*, **280**, 4149-4164.

25. Rawat,R., Cohen,T.V., Ampong,B., Francia,D., Henriques-Pons,A., Hoffman,E.P., Nagaraju,K. (2010) Inflammasome up-regulation and activation in dysferlin-deficient skeletal muscle. *Am. J. Pathol.*, **176**, 2891-2900.

26. Angelini,C., Peterle,E., Gaiani,A., Bortolussi,L., Borsato,C. (2011) Dysferlinopathy course and sportive activity: clues for possible treatment. *Acta Myol.*, **30**, 127-132.

27. Biondi,O., Villemeur,M., Marchand,A., Chretien,F., Bourg,N., Gherardi,R.K., Richard,I., Authier,F.J. (2013) Dual effects of exercise in dysferlinopathy. *Am. J. Pathol.*, **182**, 2298-2309.

28. Confalonieri,P., Oliva,L., Andreetta,F., Lorenzoni,R., Dassi,P., Mariani,E., Morandi,L., Mora,M., Cornelio,F., Mantegazza,R. (2003) Muscle inflammation and MHC class I up-regulation in muscular dystrophy with lack of dysferlin: an immunopathological study. *J. Neuroimmunol.*, **142**, 130-136.

29. Nemoto,H., Konno,S., Nakazora,H., Miura,H., Kurihara,T. (2007) Histological and immunohistological changes of the skeletal muscles in older SJL/J mice. *Eur. Neurol.*, **57**, 19-25.

30. Swirski,F.K., Nahrendorf,M., Etzrodt,M., Wildgruber,M., Cortez-Retamozo,V., Panizzi,P., Figueiredo,J.L., Kohler,R.H., Chudnovskiy,A., Waterman,P.*, et al.* (2009) Identification of splenic reservoir monocytes and their deployment to inflammatory sites. *Science*, **325**, 612-616.

31. de,L.N., Gallardo,E., Sonnet,C., Chazaud,B., Dominguez-Perles,R., Suarez-Calvet,X., Gherardi,R.K., Illa,I. (2010) Role of thrombospondin 1 in macrophage inflammation in dysferlin myopathy. *J. Neuropathol. Exp. Neurol.*, **69**, 643-653.

32. Nemoto,H., Konno,S., Sugimoto,H., Nakazora,H., Nomoto,N., Murata,M., Kitazono,H., Fujioka,T. (2011) Anti-TNF therapy using etanercept suppresses degenerative and inflammatory changes in skeletal muscle of older SJL/J mice. *Exp. Mol. Pathol.*, **90**, 264-270.

33. Han,R., Frett,E.M., Levy,J.R., Rader,E.P., Lueck,J.D., Bansal,D., Moore,S.A., Ng,R., Beltran-Valero de,B.D., Faulkner,J.A., Campbell,K.P. (2010) Genetic ablation of complement C3 attenuates muscle pathology in dysferlin-deficient mice. *J. Clin. Invest*, **120**, 4366-4374.

34. Walter,M.C., Reilich,P., Thiele,S., Schessl,J., Schreiber,H., Reiners,K., Kress,W., Muller-Reible,C., Vorgerd,M., Urban,P.*, et al.* (2013) Treatment of dysferlinopathy with deflazacort: a double-blind, placebo-controlled clinical trial. *Orphanet. J. Rare. Dis.*, **8**, 26.

35. Farini,A., Sitzia,C., Navarro,C., D'Antona,G., Belicchi,M., Parolini,D., Del,F.G., Razini,P., Bottinelli,R., Meregalli,M., Torrente,Y. (2012) Absence of T and B lymphocytes modulates dystrophic features in dysferlin deficient animal model. *Exp. Cell Res.*, **318**, 1160-1174.

36. Uaesoontrachoon,K., Cha,H.J., Ampong,B., Sali,A., Vandermeulen,J., Wei,B., Creeden,B., Huynh,T., Quinn,J., Tatem,K.*, et al.* (2013) The effects of MyD88 deficiency

on disease phenotype in dysferlin-deficient A/J mice: role of endogenous TLR ligands. *J. Pathol.*, **231**, 199-209.

37. Lennon,N.J., Kho,A., Bacskai,B.J., Perlmutter,S.L., Hyman,B.T., Brown,R.H., Jr. (2003) Dysferlin interacts with annexins A1 and A2 and mediates sarcolemmal wound-healing. *J. Biol. Chem.*, **278**, 50466-50473.

38. Kesari,A., Fukuda,M., Knoblach,S., Bashir,R., Nader,G.A., Rao,D., Nagaraju,K., Hoffman,E.P. (2008) Dysferlin deficiency shows compensatory induction of Rab27A/Slp2a that may contribute to inflammatory onset. *Am. J. Pathol.*, **173**, 1476-1487.

39. Defour,A., Sreetama,S.C., Jaiswal,J.K. (2014) Imaging cell membrane injury and subcellular processes involved in repair. *J. Vis. Exp.*, **85**, e51106.

40. Scheffer,L.L., Sreetama,S.C., Sharma,N., Medikayala,S., Brown,K.J., Defour,A., Jaiswal,J.K. (2014) Mechanism of Ca(2)(+)-triggered ESCRT assembly and regulation of cell membrane repair. *Nat. Commun.*, **5**, 5646.

41. von der,H.M., Laval,S.H., Cree,L.M., Haldane,F., Pocock,M., Wappler,I., Peters,H., Reitsamer,H.A., Hoger,H., Wiedner,M.*, et al.* (2005) The differential gene expression profiles of proximal and distal muscle groups are altered in pre-pathological dysferlin-deficient mice. *Neuromuscul. Disord.*, **15**, 863-877.

42. Wenzel,K., Zabojszcza,J., Carl,M., Taubert,S., Lass,A., Harris,C.L., Ho,M., Schulz,H., Hummel,O., Hubner,N.*, et al.* (2005) Increased susceptibility to complement attack due to down-regulation of decay-accelerating factor/CD55 in dysferlin-deficient muscular dystrophy. *J. Immunol.*, **175**, 6219-6225.

43. Turk,R., Sterrenburg,E., van der Wees,C.G., de Meijer,E.J., de Menezes,R.X., Groh,S., Campbell,K.P., Noguchi,S., van Ommen,G.J., den Dunnen,J.T., 't Hoen,P.A. (2006) Common pathological mechanisms in mouse models for muscular dystrophies. *FASEB J.*, **20**, 127-129.

44. Han,R. (2011) Muscle membrane repair and inflammatory attack in dysferlinopathy. *Skelet. Muscle*, **1**, 10.

45. Swisher,J.F., Burton,N., Bacot,S.M., Vogel,S.N., Feldman,G.M. (2010) Annexin A2 tetramer activates human and murine macrophages through TLR4. *Blood*, **115**, 549-558.

46. Ho,M., Post,C.M., Donahue,L.R., Lidov,H.G., Bronson,R.T., Goolsby,H., Watkins,S.C., Cox,G.A., Brown,R.H., Jr. (2004) Disruption of muscle membrane and phenotype divergence in two novel mouse models of dysferlin deficiency. *Hum. Mol. Genet.*, **13**, 1999-2010.

47. Lerario,A., Cogiamanian,F., Marchesi,C., Belicchi,M., Bresolin,N., Porretti,L., Torrente,Y. (2010) Effects of rituximab in two patients with dysferlin-deficient muscular dystrophy. *BMC. Musculoskelet. Disord.*, **11**, 157.

48. MacPherson,R.E., Peters,S.J. (2015) Piecing together the puzzle of perilipin proteins and skeletal muscle lipolysis. *Appl. Physiol Nutr. Metab*, **40**, 641-651.

49. Demonbreun,A.R., McNally,E.M. (2016) Plasma Membrane Repair in Health and Disease. *Curr. Top. Membr.*, **77**, 67-96.

50. McDade,J.R., Archambeau,A., Michele,D.E. (2014) Rapid actin-cytoskeleton-dependent recruitment of plasma membrane-derived dysferlin at wounds is critical for muscle membrane repair. *FASEB J.*, **28**, 3660-3670.

51. Siever,D.A., Erickson,H.P. (1997) Extracellular annexin II. *Int. J. Biochem. Cell Biol.*, **29**, 1219-1223.

52. Tsukamoto,H., Tanida,S., Ozeki,K., Ebi,M., Mizoshita,T., Shimura,T., Mori,Y., Kataoka,H., Kamiya,T., Fukuda,S*., et al.* (2013) Annexin A2 regulates a disintegrin and metalloproteinase 17-mediated ectodomain shedding of pro-tumor necrosis factor-alpha in monocytes and colon epithelial cells. *Inflamm. Bowel. Dis.*, **19**, 1365-1373.

53. Mariano,A., Henning,A., Han,R. (2013) Dysferlin-deficient muscular dystrophy and innate immune activation. *FEBS J.*, **280**, 4165-4176.

54. Scaffidi,P., Misteli,T., Bianchi,M.E. (2002) Release of chromatin protein HMGB1 by necrotic cells triggers inflammation. *Nature*, **418**, 191-195.

55. Demonbreun,A.R., Rossi,A.E., Alvarez,M.G., Swanson,K.E., Deveaux,H.K., Earley,J.U., Hadhazy,M., Vohra,R., Walter,G.A., Pytel,P., McNally,E.M. (2014) Dysferlin and myoferlin regulate transverse tubule formation and glycerol sensitivity. *Am. J. Pathol.*, **184**, 248-259.

56. Brooks,S.V., Faulkner,J.A. (1988) Contractile properties of skeletal muscles from young, adult and aged mice. *J. Physiol. (Lond.)*, **404**, 71-82.

57. Spurney,C.F., Gordish-Dressman,H., Guerron,A.D., Sali,A., Pandey,G.S., Rawat,R., Van der Meulen,J.H., Cha,H.J., Pistilli,E.E., Partridge,T.A*., et al.* (2009) Preclinical drug trials in the mdx mouse: assessment of reliable and sensitive outcome measures. *Muscle Nerve*, **39**, 591-602.

58. Gentleman,R.C., Carey,V.J., Bates,D.M., Bolstad,B., Dettling,M., Dudoit,S., Ellis,B., Gautier,L., Ge,Y., Gentry,J*., et al.* (2004) Bioconductor: open software development for computational biology and bioinformatics. *Genome Biol.*, **5**, R80.

59. Bolstad,B.M., Collin,F., Simpson,K.M., Irizarry,R.A., Speed,T.P. (2004) Experimental design and low-level analysis of microarray data. *Int. Rev. Neurobiol.*, **60**, 25-58.

60. Bolstad,B.M., Irizarry,R.A., Astrand,M., Speed,T.P. (2003) A comparison of normalization methods for high density oligonucleotide array data based on variance and bias. *Bioinformatics.*, **19**, 185-193.

61. Clark,N.R., Hu,K.S., Feldmann,A.S., Kou,Y., Chen,E.Y., Duan,Q., Ma'ayan,A. (2014) The characteristic direction: a geometrical approach to identify differentially expressed genes. *BMC. Bioinformatics.*, **15**, 79.

62. Sharov,A.A., Dudekula,D.B., Ko,M.S. (2005) A web-based tool for principal component and significance analysis of microarray data. *Bioinformatics.*, **21**, 2548-2549.

63. Saeed,A.I., Sharov,V., White,J., Li,J., Liang,W., Bhagabati,N., Braisted,J., Klapa,M., Currier,T., Thiagarajan,M.*, et al.* (2003) TM4: a free, open-source system for microarray data management and analysis. *BioTechniques*, **34**, 374-378.

64. Subramanian,A., Tamayo,P., Mootha,V.K., Mukherjee,S., Ebert,B.L., Gillette,M.A., Paulovich,A., Pomeroy,S.L., Golub,T.R., Lander,E.S., Mesirov,J.P. (2005) Gene set enrichment analysis: a knowledge-based approach for interpreting genome-wide expression profiles. *Proc. Natl. Acad. Sci. U. S. A*, **102**, 15545-15550.

65. Smoot,M., Ono,K., Ideker,T., Maere,S. (2011) PiNGO: a Cytoscape plugin to find candidate genes in biological networks. *Bioinformatics.*, **27**, 1030-1031.

66. Merico,D., Isserlin,R., Stueker,O., Emili,A., Bader,G.D. (2010) Enrichment map: a network-based method for gene-set enrichment visualization and interpretation. *PLoS. ONE.*, **5**, e13984.

67. Chen,E.Y., Tan,C.M., Kou,Y., Duan,Q., Wang,Z., Meirelles,G.V., Clark,N.R., Ma'ayan,A. (2013) Enrichr: interactive and collaborative HTML5 gene list enrichment analysis tool. *BMC. Bioinformatics.*, **14**, 128.

FIGURES

Figure 1: Lack of AnxA2 causes poor sarcolemmal repair. **(A)** Freshly isolated intact *Soleus* (SOL) muscle isolated from WT or A2 mice were injured *ex vivo* in presence of FM1-43 dye. The images show time lapse images of fibers visualized for brightfield (pre injury, left panel), and for fluorescence emission of the FM dye pre and post injury (middle, right panels). Individual myofibers are marked by dotted white line, and arrows indicated the site of sarcolemmal injury. Scale bar = 20 μm. **(B)** Quantification of FM1-43 influx, following laser injury, into fiber isolated from WT in presence (n = 14 fibers) or absence of calcium (n = 4 fibers) and AnxA2 deficient (n = 22 fibers) mice. **(C)** Percentage of initial force as a result of repeated 10% *ex vivo* lengthening contractions of WT or A2 *Extensor Digitorum Longus* (EDL) muscle from 1 year old animal (n = 3-4 animals each). **(D)** Percentage of initial force as a result of repeated 10% *ex vivo* lengthening contractions of WT or A2 SOL muscle from 1 year old animal (n = 3 animals each). **(E)** Cross-section of EDL muscle section stained with procion orange following 10 repeated lengthening contractions in WT and A2 from 1 year old animal: brightfield (left panel) and procion orange (right panel). Scale bar = 50 μm. All images were acquired and scaled similarly and quantifications show means ± S.E.M. B: ** $p \leq 0.01$ and *** $p \leq 0.001$ compared to WT and ### $p \leq 0.001$ compared to A2 by ANOVA ; C : * $p \leq 0.05$ compared to WT by unpaired t-test.

Figure 2: AnxA2 deficient mice show progressive muscle weakness and decline in locomotor activity. A2 and parental WT mice at different ages (3 to 24 months old) were assessed for muscle strength and voluntary locomotor activity. **(A)** Forelimb grip strength measurement (GSM). **(B)** Specific force of isolated *Extensor Digitorum Longus* (EDL) muscle. **(C - E)** Voluntary locomotor activity assessed by open-field behavior measurements. All data are

expressed as medians ± extreme values through whisker plot (n > 9 animals). * $p \leq 0.05$, ** $p \leq 0.01$ and *** $p \leq 0.001$ compared to WT by unpaired t-test.

Figure 3: Annexin A2 deficit does not increase muscle degeneration and inflammation. *Gastrocnemius* (GSC) muscle sections from A2, WT and dysferlin deficient (B6A/J) mice at different ages (3, 6 and 9 months old) were stained with haematoxylin & eosin (H&E) and various histological features were quantified. **(A)** Representative histological images of GSC muscle for WT, A2 and B6A/J mice. **(B)** H&E stained muscle sections were imaged from >4 independent animals and the entire muscle section was used to quantify the number of **(B)** degenerated fibers (open arrow), **(C)** inflammatory foci (white arrow) and **(D)** centrally nucleated fibers (black arrow). Scale bar = 100 µm. All data are expressed as mean ± S.E.M (n > 4 animals). * $p \leq 0.05$ and** $p \leq 0.01$ compared to WT and # $p \leq 0.05$ compared to A2 by Kruskal Wallis test.

Figure 4: Lack of AnxA2 reduces muscle inflammation in dysferlinopathic mouse. B6A/J and B6A/JA2 mice at 6-24 months of age were assessed for **(A)** body mass and **(B, C)** muscle mass (*Gastrocnemius*, GSC or *Tibialis Anterior*, TA), as well as **(D)** the ability of the myofiber from *Extensor Digitorum Longus* (EDL) or *biceps* muscle of B6A/J (n = 13 fibers) or B6A/JA2 (n = 15 fibers) mice to repair from laser injury *ex vivo*. **(E)** Representative histological images of the haematoxylin & eosin stained EDL muscle cross section from WT, A2, B6A/J and B6A/JA2 at 24 months old. Scale bar = 100 µm. Number of **(F)** degenerating muscle fibers (open arrow), **(G)** inflammatory foci (white arrow) and **(H)** central nucleated fibers (black arrow) were quantified from entire EDL muscles of WT, A2, B6A/J and B6A/JA2 at 24 months of age (n > 3 animals). **(I, J)** mRNA expression level (normalized to HPRT and presented as fold-change over

the WT) for **(I)** various inflammatory cell population and **(J)** genes involved in TLR-signaling response in A2, B6A/J or B6A/JA2 GSC muscle at 24 months (n > 3 animals). All data are expressed as means ± S.E.M. $$ $p \leq 0.01$ compared to B6A/J by unpaired t-test. * $p \leq 0.05$ and ** $p \leq 0.01$ compared to WT and ## $p \leq 0.01$ compared to A2 by Kruskal Wallis test.

Figure 5: Lack of AnxA2 reduces fatty replacement of dysferlinopathic muscles. *Gastrocnemius* muscle from 12 month old WT, A2, B6A/J and B6A/JA2 mice were stained with **(A)** haematoxylin & eosin, **(B)** Oil Red O and **(C)** immunostained for Perilipin1 (red). Scale = 200 μm for A & B and 100 μm for C. **(D)** Using images of whole muscle section the number of perlilipin1 stained foci were quantified (n = 3 animals each). Blue: DAPI, Green: Wheat germ Agglutinin (Alexa Fluor 488 conjugate), and Red: Perilipin1 (Alexa fluor 568 conjugate).The plots represent mean ± SEM. * $p \leq 0.05$ compared to WT by Kruskal Wallis test.

Figure 6: Lack of AnxA2 improves dysferlinopathic muscle function. (A, B). Forelimb and hindlimb grip strength (GSM) measurement of B6A/J or B6A/JA2 mice at < 6 months and WT, B6A/J or B6A/JA2 at > 20 months (n > 10 animals). **(C)** Percentage of initial force as a result of successive 10% *ex vivo* lengthening contractions of B6A/J or B6A/JA2 *Extensor Digitorum Longus* (EDL) muscle from 6 months or 1 year old animal (n > 4 animals). **(D)** Specific force of EDL muscle from B6A/J or B6A/JA2 mice at 6, 12 and 24 months (n > 6 animals). **(E-G)** Voluntary locomotor activity assessed by open-field behavioral activity measurements of B6A/J or B6A/JA2 mice at < 6 months and WT, B6A/J or B6A/JA2 mice at > 20 months (n > 10 animals). Box whisker plots show median ± extreme values, while line plot (C) shows means ± S.E.M. A, B, E-G : * $p \leq 0.05$ and *** $p \leq 0.001$ compared to WT and $ $p \leq 0.05$, $$ $p \leq 0.01$

and $$$ ≤ 0.001 compared to B6A/J by Kruskal Wallis test ; C : * p ≤ 0.05, ** p ≤ 0.01 and *** p ≤ 0.001 compared to B6A/J by ANOVA.

Table S1: Microarray probe sets showing differential expression (FDR q-value < 0.1) in A2 muscles as compared to age matched parental WT muscle.

Symbol	Fold-Change	P-value	FDR
AnxA2	-2.67	0	0
Nedd4	5.75	0	0.00273
Ppcdc	-1.87	0	0.00273
2210418O10Rik	-1.61	0.00001	0.04454
Tpm1	2.06	0.00001	0.04454
Dynlt1a|Dynlt1b|Dynlt1c|Dynlt1f	1.85	0.00001	0.04836

Table S2: Enrichment of inflammation-related and fat-related gene ontology terms among the 250 most differentially expressed genes (as compared against their respective wild-type controls) in muscle of the 6 months old A2 murine model and from datasets of dysferlin-deficient murine muscles at 7 months (GSE2507), 2 months (GSE2112), or 1 month (GSE2629_QF, GSE2629_TA) of age; P-values of 0.1 or less are shown, while the rest were considered not significant (NS). *For fat-related gene ontology terms, an additional dataset (GSE51866) for fat tissue vs muscle tissue was included for comparison.

	A2	Dysferlin-deficient				Fat *versus* muscle (GSE51866)*
		GSE2507	GSE2112	GSE2629_QF	GSE2629_TA	
Inflammation-related Gene Ontology terms						
Inflammatory response	NS	NS	0.002	0.002	0.001	
Regulation of inflammatory response	NS	0.003	0.001	0.009	0.007	
Positive regulation of inflammatory response	NS	0.009	0.016	0.087	0.003	
Activation of innate immune response	NS	0.002	NS	NS	0.003	
Activation of immune response	NS	0.010	NS	NS	NS	
Adaptive immune response	NS	0.002	0.075	0.094	NS	
Positive regulation of innate immune response	NS	0.006	NS	NS	0.012	
Adipose-related Gene Ontology terms						
Brown fat cell differentiation	NS	0.079	NS	NS	0.017	< 0.001
Fatty acid metabolic process	NS	0.019	NS	NS	NS	0.016
Fatty acid oxidation	NS	0.003	NS	NS	NS	0.060

ABBREVIATIONS

Annexin (Anx), danger associated molecular patterns (DAMP), differentially expressed genes (DEG), *Extensor Digitorum Longus* (EDL), false discovery rate (FDR), gene expression omnibus (GEO), gene oncology (GO), *Gastrocnemius* (GSC), grip strength meter (GSM), haematoxylin and eosin (H&E), high mobility group (HMG), lengthening contraction (LC), Limb Girdle Muscular Dystrophy (LGMD), Miyoshi Myopathy (MM), principal component analysis (PCA), plasma membrane (PM), *Psoas* (PSO), *Soleus* (SOL), *Tibialis Anterior* (TA), toll-like receptor (TLR) and wild type (WT).

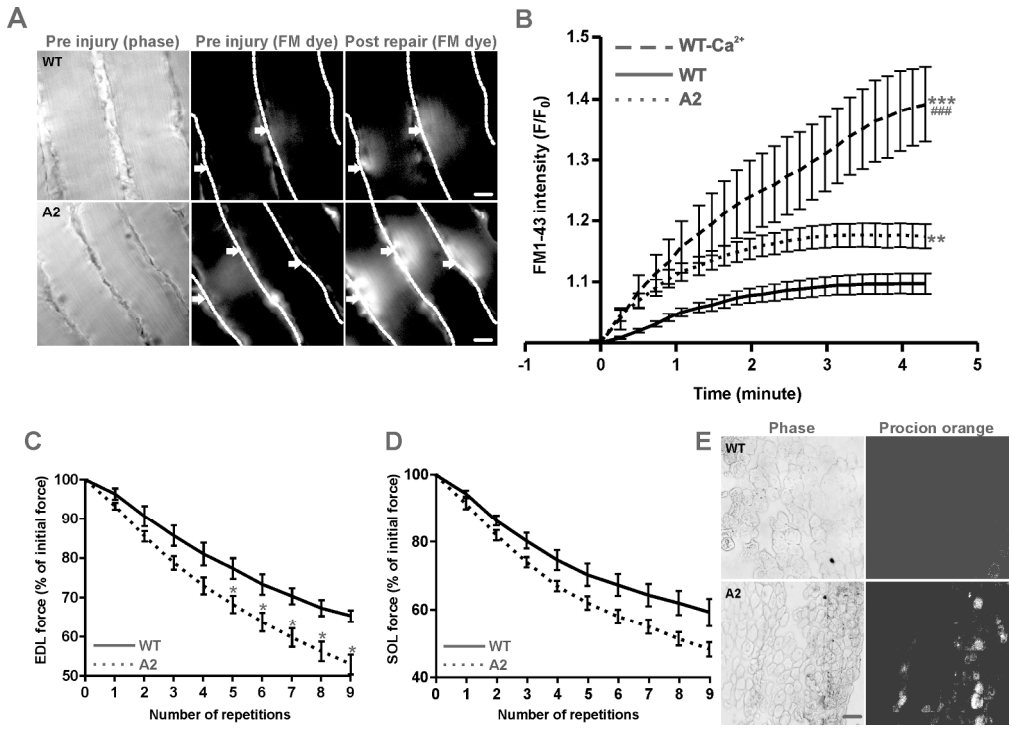

Figure 1: Lack of AnxA2 causes poor sarcolemmal repair. (A) Freshly isolated intact Soleus (SOL) muscle isolated from WT or A2 mice were injured in presence of FM1-43 dye. The images show time lapse images of fibers visualized for brightfield (pre injury, left panel), and for fluorescence emission of the FM dye pre and post injury (middle, right panels). Individual myofibers are marked by dotted white line, and arrows indicated the site of sarcolemmal injury. Scale bar = 20 μm. (B) Quantification of FM1-43 influx, following laser injury, into fiber isolated from WT in presence (n = 14 fibers) or absence of calcium (n = 4 fibers) and AnxA2 deficient (n = 22 fibers) mice. (C) Percentage of initial force as a result of repeated 10% lengthening contractions of WT or A2 Extensor Digitorum Longus (EDL) muscle from 1 year old animal (n = 3-4 animals each). (D) Percentage of initial force as a result of repeated 10% lengthening contractions of WT or A2 SOL muscle from 1 year old animal (n = 3 animals each). (E) Cross-section of EDL muscle section stained with procion orange following 10 repeated lengthening contractions in WT and A2 from 1 year old animal: brightfield (left panel) and procion orange (right panel). Scale bar = 50 μm. All images were acquired and scaled similarly and quantifications show means ± S.E.M. B: ** $p \leq 0.01$ and *** $p \leq 0.001$ compared to WT and ### $p \leq 0.001$ compared to A2 by ANOVA ; C : * $p \leq 0.05$ compared to WT by unpaired t-test.

Fig. 1

221x158mm (300 x 300 DPI)

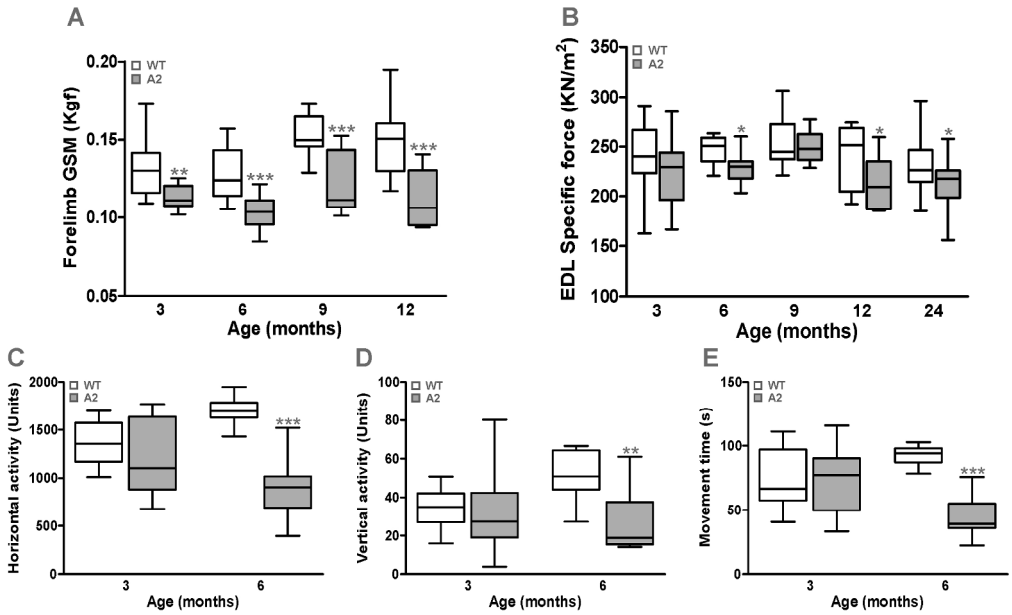

Figure 2: AnxA2 deficient mice show progressive muscle weakness and decline in locomotor activity. A2 and parental WT mice at different ages (3 to 24 months old) were assessed for muscle strength and voluntary locomotor activity. (A) Forelimb grip strength measurement (GSM). (B) Specific force of isolated Extensor Digitorum Longus (EDL) muscle. (C - E) Voluntary locomotor activity assessed by open-field behavior measurements. All data are expressed as medians ± extreme values through whisker plot (n > 9 animals). * $p \leq 0.05$, ** $p \leq 0.01$ and *** $p \leq 0.001$ compared to WT by unpaired t-test.

Fig. 2

223x134mm (300 x 300 DPI)

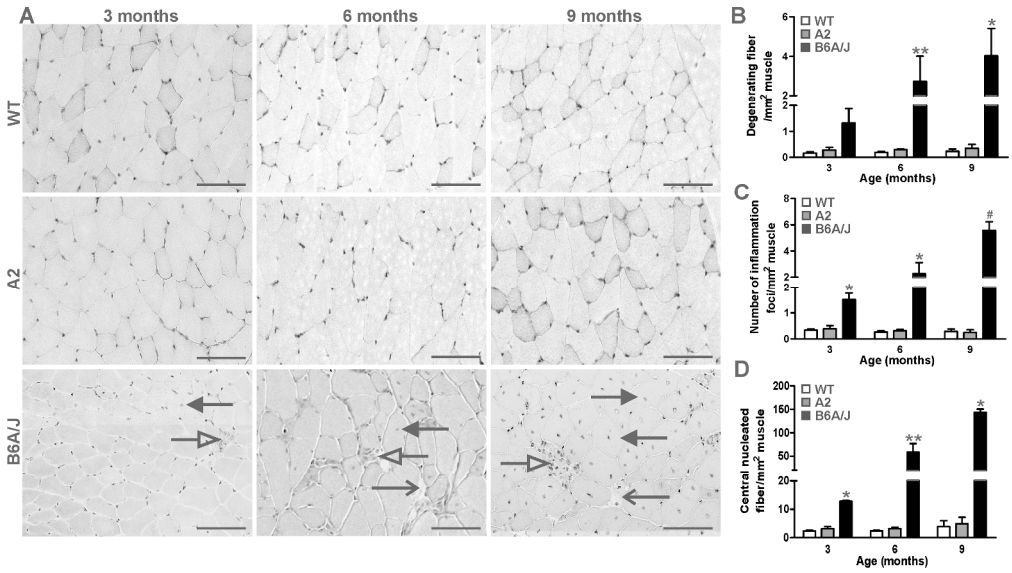

Figure 3: Annexin A2 deficit does not increase muscle degeneration and inflammation. Gastrocnemius (GSC) muscle sections from A2, WT and dysferlin deficient (B6A/J) mice at different ages (3, 6 and 9 months old) were stained with haematoxylin & eosin (H&E) and various histological features were quantified. (A) Representative histological images of GSC muscle for WT, A2 and B6A/J mice. (B) H&E stained muscle sections were imaged from >4 independent animals and the entire muscle section was used to quantify the number of (B) degenerated fibers (open arrow), (C) inflammatory foci (white arrow) and (D) centrally nucleated fibers (black arrow). Scale bar = 100 µm. All data are expressed as mean ± S.E.M (n > 4 animals). * $p \leq 0.05$ and** $p \leq 0.01$ compared to WT and # $p \leq 0.05$ compared to A2 by Kruskal Wallis test.

Fig. 3

250x140mm (300 x 300 DPI)

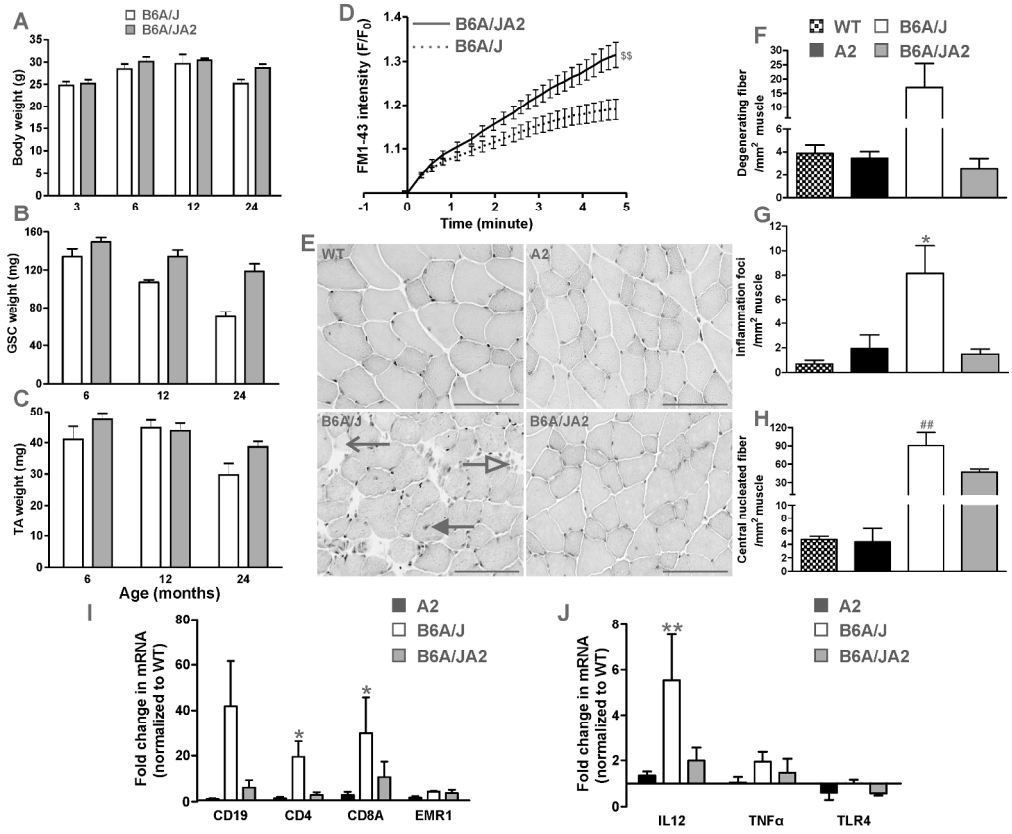

Figure 4: Lack of AnxA2 reduces muscle inflammation in dysferlinopathic mouse. B6A/J and B6A/JA2 mice at 6-24 months of age were assessed for (A) body mass and (B, C) muscle mass (Gastrocnemius, GSC or Tibialis Anterior, TA), as well as (D) the ability of the myofiber from Extensor Digitorum Longus (EDL) or biceps muscle of B6A/J (n = 13 fibers) or B6A/JA2 (n = 15 fibers) mice to repair from laser injury ex vivo. (E) Representative histological images of the haematoxylin & eosin stained EDL muscle cross section from WT, A2, B6A/J and B6A/JA2 at 24 months old. Scale bar = 100 µm. Number of (F) degenerating muscle fibers (open arrow), (G) inflammatory foci (white arrow) and (H) central nucleated fibers (black arrow) were quantified from entire EDL muscles of WT, A2, B6A/J and B6A/JA2 at 24 months of age (n > 3 animals). (I, J) mRNA expression level (normalized to HPRT and presented as fold-change over the WT) for (I) various inflammatory cell population and (J) genes involved in TLR-signaling response in A2, B6A/J or B6A/JA2 GSC muscle at 24 months (n > 3 animals). All data are expressed as means ± S.E.M. $$ $p \leq 0.01$ compared to B6A/J by unpaired t-test. * $p \leq 0.05$ and ** $p \leq 0.01$ compared to WT and ## $p \leq 0.01$ compared to A2 by Kruskal Wallis test.

Fig. 4

246x202mm (300 x 300 DPI)

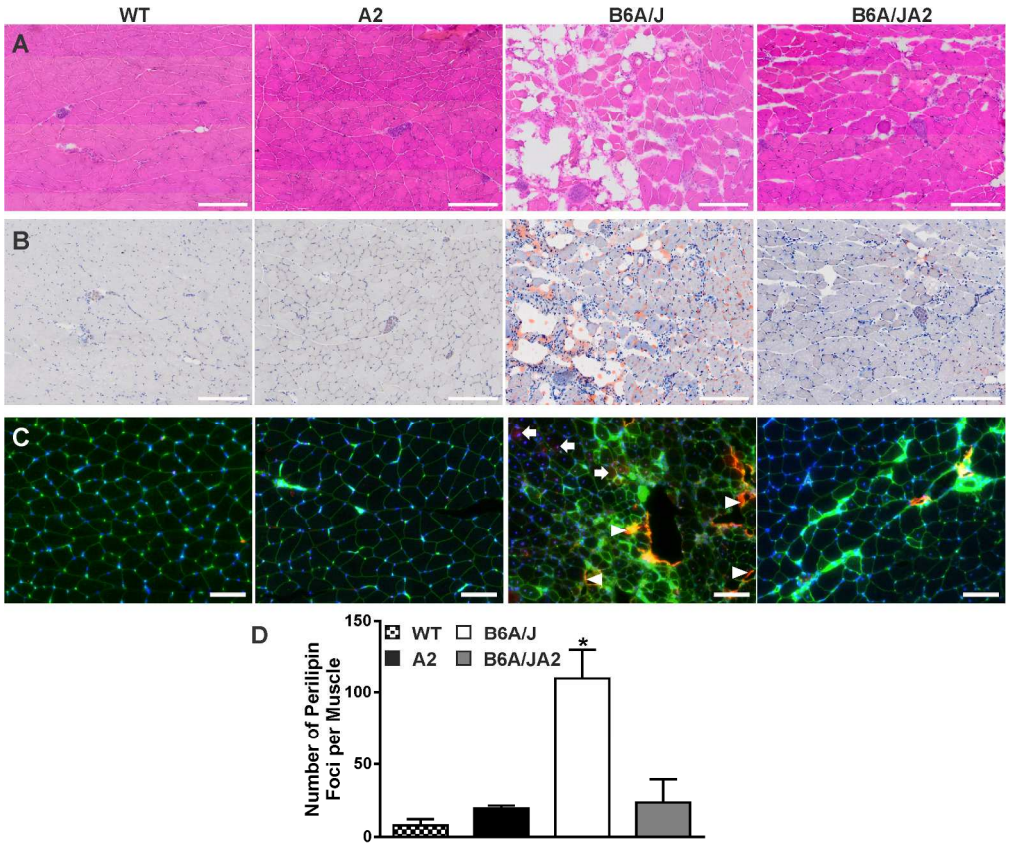

Figure 5: Lack of AnxA2 reduces fatty replacement of dysferlinopathic muscles. Gastrocnemius muscle from 12 month old WT, A2, B6A/J and B6A/JA2 mice were stained with (A) haematoxylin & eosin, (B) Oil Red O and (C) immunostained for Perilipin1 (red). Scale = 200 μm for A & B and 100 μm for C. (D) Using images of whole muscle section the number of perlilipin1 stained foci were quantified (n = 3 animals each). Blue: DAPI, Green: Wheat germ Agglutinin (Alexa Fluor 488 conjugate), and Red: Perilipin1 (Alexa fluor 568 conjugate).The plots represent mean ± SEM. * $p \leq 0.05$ compared to WT by Kruskal Wallis test.

Fig. 5

224x186mm (300 x 300 DPI)

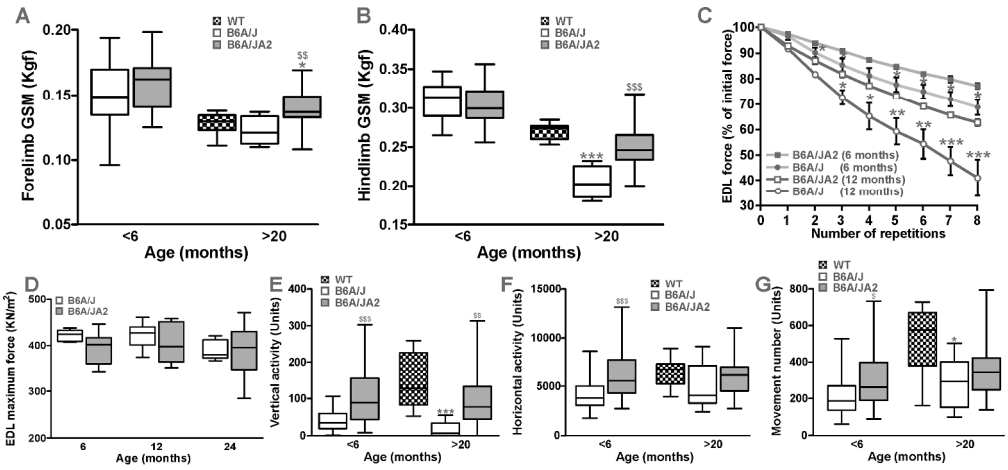

Figure 6: Lack of AnxA2 improves dysferlinopathic muscle function. (A, B). Forelimb and hindlimb grip strength (GSM) measurement of B6A/J or B6A/JA2 mice at < 6 months and WT, B6A/J or B6A/JA2 at > 20 months (n > 10 animals). (C) Percentage of initial force as a result of successive 10% lengthening contractions of B6A/J or B6A/JA2 Extensor Digitorum Longus (EDL) muscle from 6 months or 1 year old animal (n > 4 animals). (D) Specific force of EDL muscle from B6A/J or B6A/JA2 mice at 6, 12 and 24 months (n > 6 animals). (E-G) Voluntary locomotor activity assessed by open-field behavioral activity measurements of B6A/J or B6A/JA2 mice at < 6 months and WT, B6A/J or B6A/JA2 mice at > 20 months (n > 10 animals). Box whisker plots show median ± extreme values, while line plot (C) shows means ± S.E.M. A, B, E-G : * $p \leq 0.05$ and *** $p \leq 0.001$ compared to WT and \$ $p \leq 0.05$, \$\$ $p \leq 0.01$ and \$\$\$ ≤ 0.001 compared to B6A/J by Kruskal Wallis test ; C : * $p \leq 0.05$, ** $p \leq 0.01$ and *** $p \leq 0.001$ compared to B6A/J by ANOVA.

Fig. 6
260x118mm (300 x 300 DPI)